FORAMINIFERAL POPULATION DYNAMICS AND STABLE CARBON ISOTOPES

Christoph Hemleben and Jelle Bijma[1]
Institut und Museum für Geologie und Paläontologie
Universität Tübingen
Sigwartstraße 10
D-72076 Tübingen

ABSTRACT. Most planktic foraminifera live within the photic zone and exhibit a life style tied to the lunar cycle. They migrate between the reproductive depth (thermocline and/or the chlorophyll maximum) and the uppermost part of the photic zone. This ontogenetic migration pattern sets the initial $\delta^{13}C$ of the foraminiferal shell. On top of that, biological fractionation processes (vital effects) modify the signal. These processes include photosynthetic activity of the symbionts and respiration of the host/symbiont complex. *Globigerinoides sacculifer* (Brady) was chosen to model ontogenetic changes in the $\delta^{13}C$ of the shell as a function of depth migration with and without vital effects.

INTRODUCTION

Reconstructions of marine paleo-environments are frequently based on stable isotope measurements. General assumptions are that a foraminifer has a rather steady life habitat throughout ontogeny and that the $\delta^{13}C$ of ΣCO_2 is constant in the mixed layer. However, because most planktic foraminifera, if not all, change their life horizon during ontogeny and because the $\delta^{13}C$ of ΣCO_2 is not necessarily constant in the mixed layer, the isotopic composition of the foraminiferal shell is not only dependent on water-mass properties (e.g. oligotrophic vs. eutrophic) and the geographic and climatic setting (e.g. upwelling, monsoon, subarctic etc.) but to an important extent on the life history of the foraminifer. Consequently, the disequilibrium precipitation of the foraminiferal shell (so called "vital effect") reported in the literature (e.g. Berger *et al.*, 1978) can often be explained in terms of ontogenetic migration and biological fractionation. In this paper we shall discuss the potential effect of

[1] Present address: Alfred Wegener Institut für Polar- und Meeresforschung, Columbusstraße, D-27570 Bremerhaven, Germany

NATO ASI Series, Vol. I 17
Carbon Cycling in the Glacial Ocean:
Constraints on the Ocean's Role in Global Change
Edited by R. Zahn et al.

some of these processes on the stable carbon isotope composition of the shell of *G. sacculifer*.

POPULATION DYNAMICS

Despite all the useful information on biostratigraphy, stable isotopes and biology of planktic foraminifera that has been compiled (for references see, e.g., Vincent and Berger, 1981) little knowledge exists on the population dynamics of planktic foraminifers (see Hemleben *et al.*, 1989). Only a few papers deal with the small scale temporal and spatial events that occur in populations.

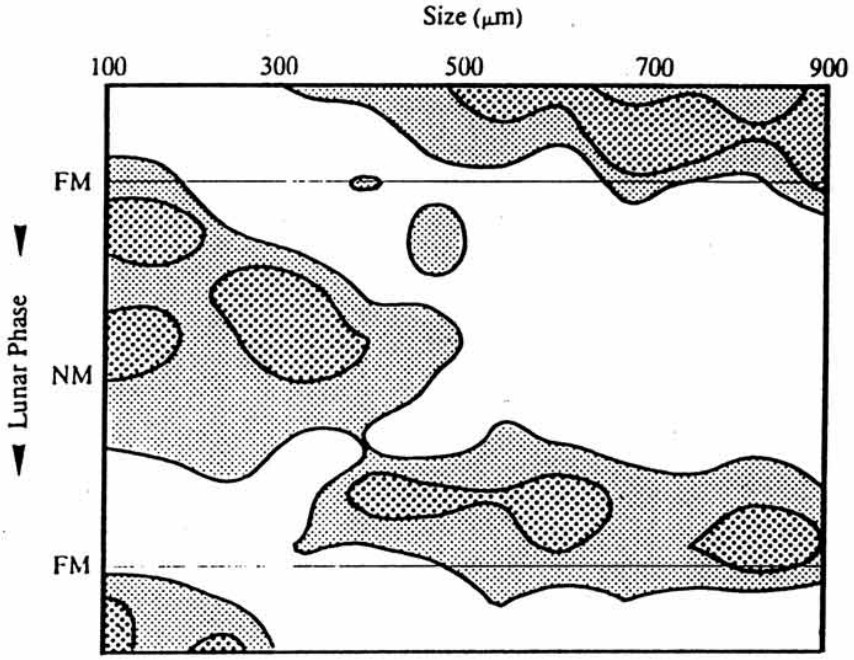

Figure 1: Lunar cycle of *G. sacculifer*. Contour plot of residual values in a size-time frame, showing that the larger size-fractions are most frequent just before full moon (FM) and that the smaller size-fractions are most frequent just after FM. Spindler *et al.* (1979).

Spindler *et al.* (1979) were the first to document that reproduction in the planktic foraminifer *Hastigerina pelagica* (d'Orbigny) is coupled to the synodic lunar cycle. Almogi-Labin (1984) has indicated that *Globigerinoides sacculifer* (Brady) reproduces at full moon in the Gulf of Elat/Aqaba. Based on a time series of plankton-net tows, a synodic lunar reproductive cycle in *G. sacculifer* (Figure 1) has been shown by Bijma *et al.* (1990) and subsequently confirmed by Erez *et al.* (1991).

Time series samples collected in the Red Sea (METEOR Cruise 5) and the northeast Atlantic Ocean (METEOR Cruise 10) demonstrate the concept of lunar cyclicity in the life cycle of other spinose planktic species, e.g. the symbiont-free, spinose species *Globigerina*

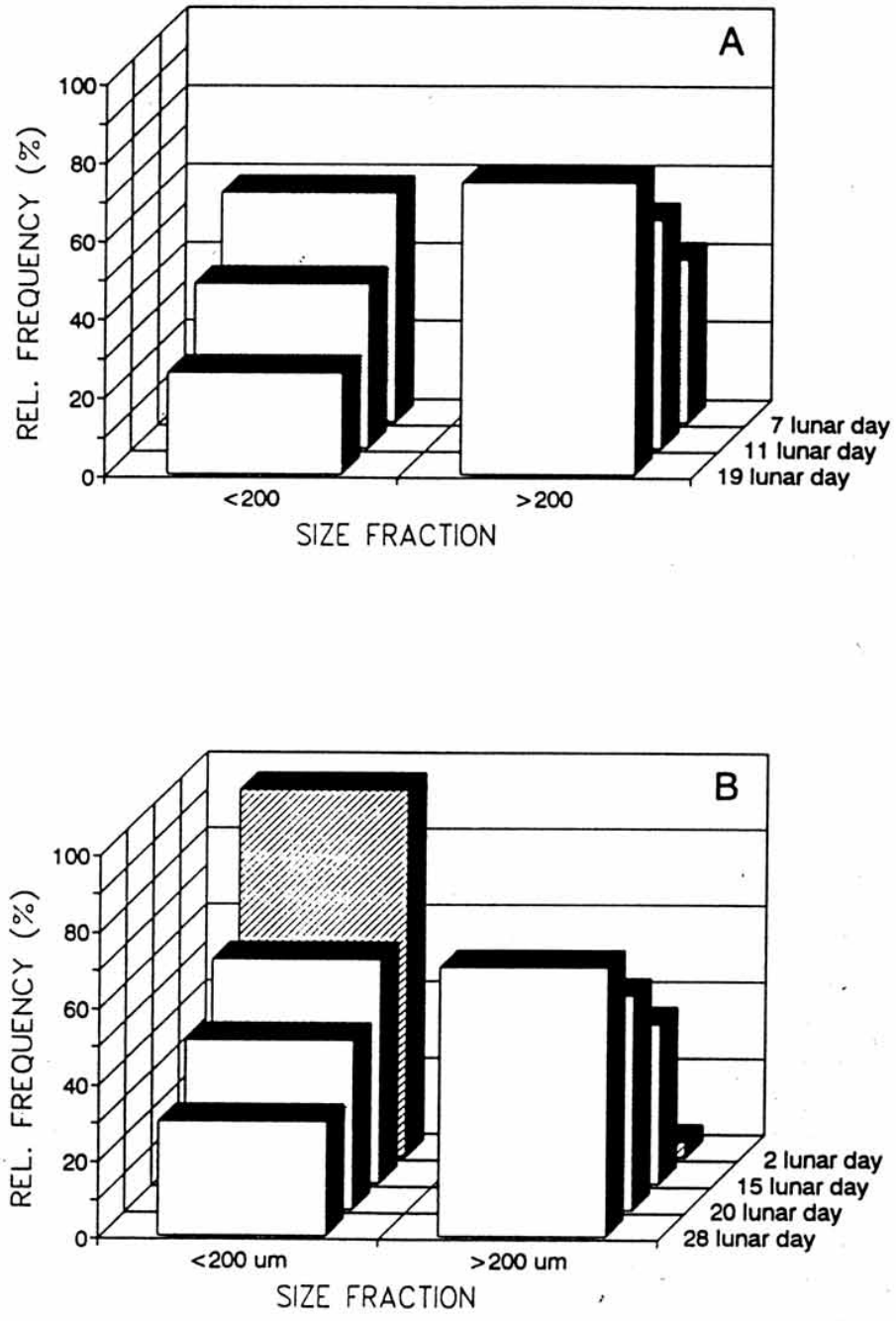

Figure 2: Relative frequency and size fraction of *G. bulloides* in respect to full moon (1. lunar day=full moon) . A: in the productive zone (0-60 m). B: in the flux zone (300-500 m).

bulloides and the symbiont bearing spinose species *Orbulina universa* (figs. 2-3). On the other hand, the deep living non-spinose foraminifers *Globorotalia scitula, G. hirsuta,* and *G. truncatulinoides* do not respond to the lunar cycle (Figure 4) and probably have a yearly life-cycle (Hemleben *et al.*, 1989). Because most spinose planktic foraminifers are associated with symbiotic algae, their main habitat is the euphotic zone. For instance, the number of *G. sacculifer* decreases drastically with depth. On the basis of absolute abundance, 95% of the shells collected in the upper 100 m of the water column live in the upper 80 m (Figure 5A). *Orbulina universa* d'Orbigny shows a subsurface maximum; and even the symbiont-barren *Globigerina bulloides* lives almost exclusively in the euphotic zone (Figure 5B-C).

The depth migration of *G. sacculifer* during ontogeny has recently been documented (Bijma and Hemleben, 1993). It was shown that this species does not inhabit a specific depth, but migrates up and down in the water column in response to its life cycle while growing (Figure 6). Thus, not only the absolute abundance changes with depth but also the size distribution changes with depth (Figure 6A). The small fraction (<300 µm) dominates the water column but their relative frequency decreases with depth until, between 60 and 80 m depth, the larger fractions (>300 µm) become dominant. Below 80 m depth, however, the small size fraction starts to dominate again. The cumulative plot of the relative frequency of mature (>366 µm) and immature specimens (<366 µm) versus water-depth (Figure 6A) demonstrates a bimodal pattern with a breakpoint between 60 to 80 m depth. The maximum of mature specimens coincides with the depth range 60 to 80 m. The relative number of immature specimens increases towards shallower and deeper environments. Apparently, reproduction in the central Red Sea takes place at approximately 60 to 80 m depth. Recruitment is shown by the ascent of immature specimens to the surface. High mortality rates in early ontogeny are probably responsible for the increase of immature specimens below the reproduction depth. The latter fraction is part of the shell flux to the sea floor.

A contour plot of the distribution of *G. sacculifer* in the productive zone demonstrates sizedependent depth preferences (Figure 6B). The plot demonstrates that the upper 20 m are the preferred habitat for immature specimens between 100 and 300 µm. The depth range between 20 and 40 m is favored by specimens from 300 to 500 µm. This is the depth where maturation takes place. Specimens between 500 and 700 µm prefer a depth range between 40 to 60 m, and specimens larger than 700 µm are found between 60 and 80 m depth, just above the reproduction depth (Figure 6B).

The depth habitat is probably dependent on the hydrological conditions and may thus differ for different water bodies. At present, we believe that the thermocline and/or the deep chlorophyll maximum determine the reproduction depth.

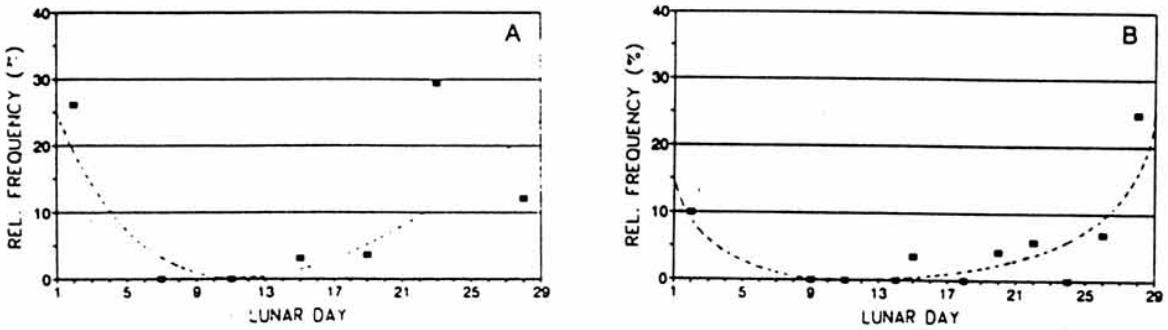

Figure 3: Relative frequency of *O. universa* in respect to the lunar period. A: in the productive zone (0-60 m). B: in the flux zone (300-500 m).

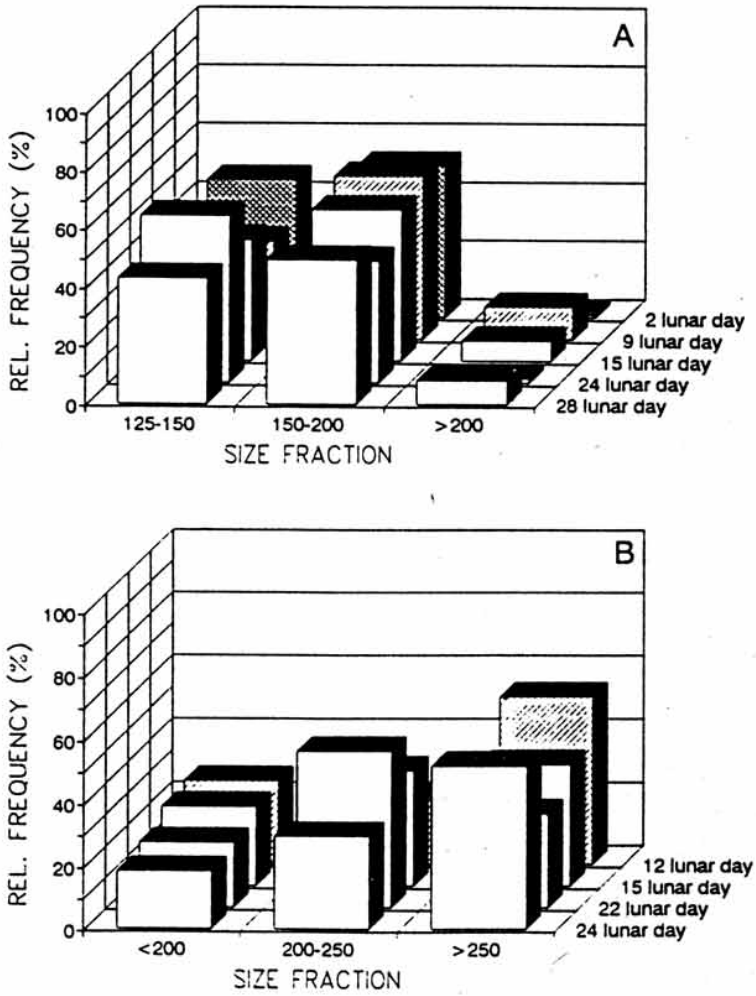

Figure 4: Non-spinose species do not respond to the lunar cycle. Samples were collected between 300-500 m depth. A: *G. scitula*. B: *G. hirsuta*.

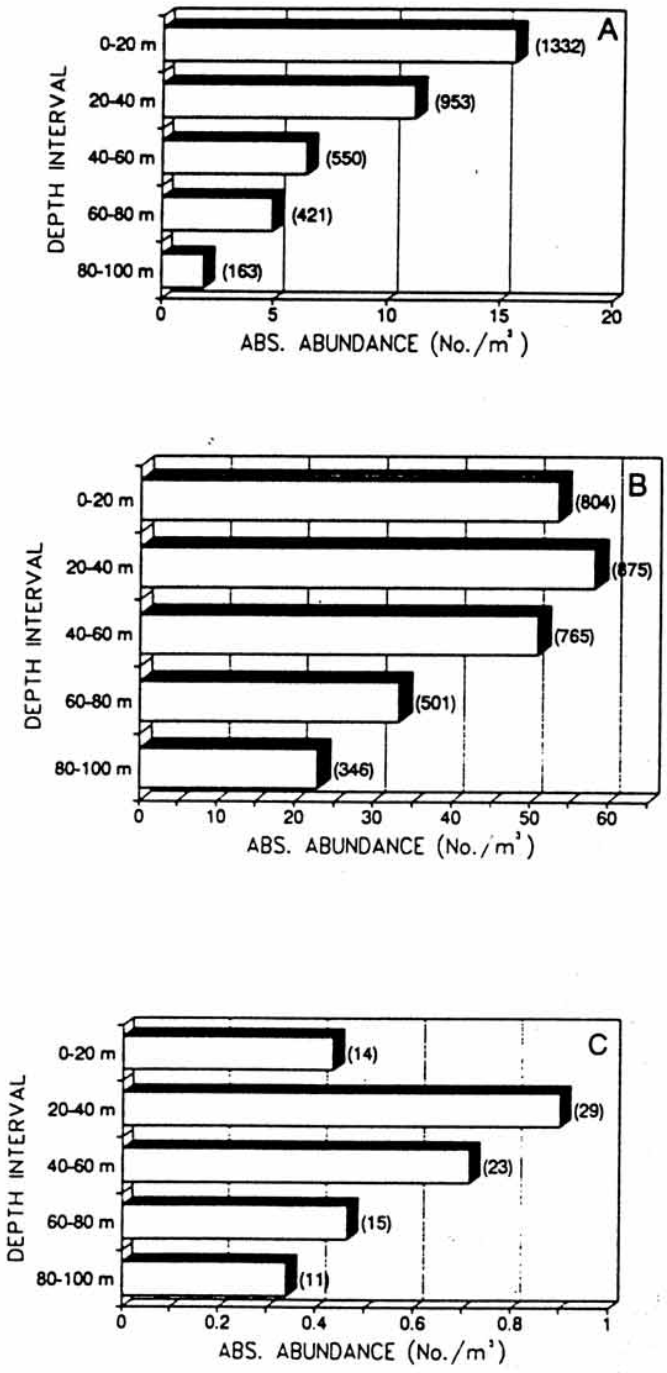

Figure 5: Mean abundance (No./m^3) of planktic foraminifers in the upper 100 m of the water column. A: *Globigerinoides sacculifer* >100 µm in the Central Red Sea. B: *Globigerina bulloides* >125 µm from the North Atlantic. C: Spherical *Orbulina universa* >125 µm from the North Atlantic. The total number of specimens are bracketed.

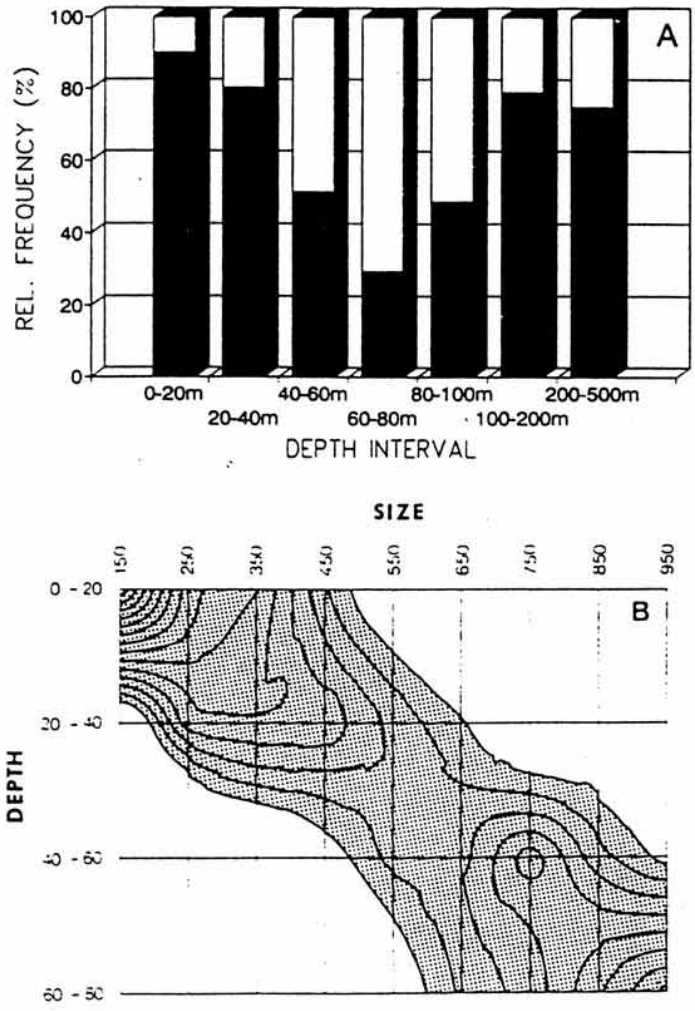

Figure 6: A: The frequency (%) of mature (>366 µm; white) and immature (<366 µm; black) *G. sacculifer* show a characteristic break between 60 and 80 m depth. B: Contour plot of residual values in a size-depth frame, showing that larger size fractions prefer deeper depth-habitats. The cross-sections of the grid represent the data points. The centers of the nine size factions (100 µm wide) and the depth intervals are listed. The shaded area contains positive residual values, indicating a larger than average presence of a size fraction. The isolines start with 0 and are drawn at 0.05 intervals. The blank area contains negative residual values, indicating a smaller than average presence of a size fraction.

$\delta^{13}C$ OF ΣCO_2 AS A FUNCTION OF DEPTH

The CO_2-fixing enzyme of most marine algae (C_3-plants), RuBP-carboxylase (ribulose-1,5bisphosphate carboxylaseoxygenase), has a higher affinity for $^{12}CO_2$ than for $^{13}CO_2$. As a result, the marine photic zone is enriched in ^{13}C relative to equilibrium with atmospheric CO_2. Simultaneously, the photosynthetically fixed carbon, which is enriched in isotopically light carbon, is decomposed by bacteria resulting in lower $\delta^{13}C$ values with depth. As a result of oxygen producing photosynthesis in the surface waters and oxygen consuming bacterial decomposition in deeper waters an empirical relationship between the $\delta^{13}C$ of the total CO_2

(ΣCO_2) and the apparent oxygen utilization (AOU) was established (Williams *et al.*, 1977). Because nutrients are utilized during photosynthesis and released by bacterial decomposition, a strong negative correlation can be seen also between the $\delta^{13}C$ of ΣCO_2 and nutrients. However, the correlation between $\delta^{13}C$ and nutrients may be disrupted (note that the surface $[PO_4]$ is less than the $[PO_4]$ at 100 m depth, yet both depth have similar $\delta^{13}C$ of ΣCO_2) due to the temperature dependence of the carbon isotope fractionation between atmospheric CO_2 and surface ocean ΣCO_2. The extent of the disruption depends on the relative strength of mixing within the sea and CO_2 exchange between ocean and atmosphere (Broecker and Maier-Reimer, 1992).

It is often assumed (e.g. Spero and Williams, 1989) that the $\delta^{13}C$ of ΣCO_2 is constant with depth in the mixed layer. This, however, is not necessarily true: In regions with a seasonal thermocline, the $\delta^{13}C$-value of ΣCO_2 is dependent on the gross assimilation rate (GAR) in the photic zone. For a station in the North Atlantic at 35°25'N, 29°30'W a subsurface $\delta^{13}C$ and oxygen maximum could be correlated to a nutrient minimum (Figure 7A-B; data courtesy Ganssen and Brummer, VU, Amsterdam). Apparently, the $\delta^{13}C$ of ΣCO_2 in the "mixed layer" cannot be assumed constant. As long as the rate of $\delta^{13}C$ enrichment through photosynthesis is faster than the rate of mixing, a $\delta^{13}C$-gradient will develop, independent of water stratification.

PREDICTING $\delta^{13}C$ OF THE FORAMINIFERAL SHELL

Already in 1978, Berger *et al.* demonstrated that $\delta^{13}C$ is dependent on the growth stage. They correlated the changing isotopic composition with environmental and metabolic signals, which are indeed the main influencing parameters. To predict the $\delta^{13}C$ of the shell of *G. sacculifer* at each ontogenetic stage under equilibrium conditions (i.e. no vital effects) we used several growth statistics. Foraminifers do not grow continuously, but by addition of separate chambers (accretionary growth). Consequently, the effect of newly formed chambers on the final isotope composition of the test can be calculated by using a mass balance equation:

$$\delta^{13}C_n = \left(\frac{W_{n-1}}{W_n}\right)\delta^{13}C_{n-1} + \left(\frac{W_n - W_{n-1}}{W_n}\right)\delta^{13}C_{water} \qquad (1)$$

where W stands for weight and n and n-1 are the nth and the (n-1)th chamber-stage. In addition, several other relationships must be known: 1) A growth relationship was derived from Figure 8 and is based on culture experiments with *G. sacculifer*,

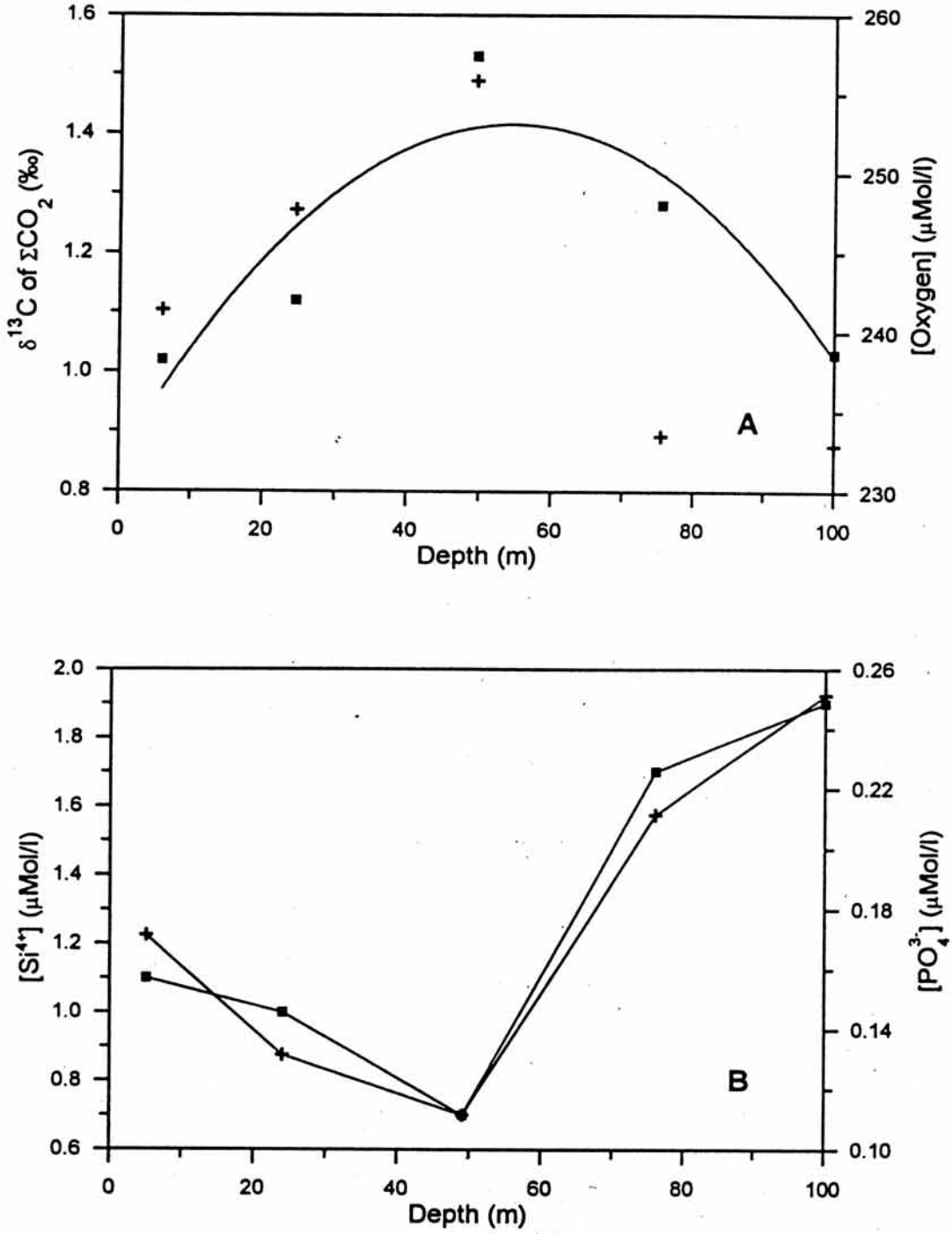

Figure 7: A: The $\delta^{13}C$ of the total dissolved CO_2 (•) and the oxygen concentration (+) at 35°25'N, 29°30'W as a function of depth. The polynom for $\delta^{13}C$ is $0.000189*depth^2 +0.0206*depth+0.853$. B: The silicium (•) and the phosphate concentration (+) at the same station (data courtesy of G. Ganssen and G.J.A. Brummer, Free University of Amsterdam).

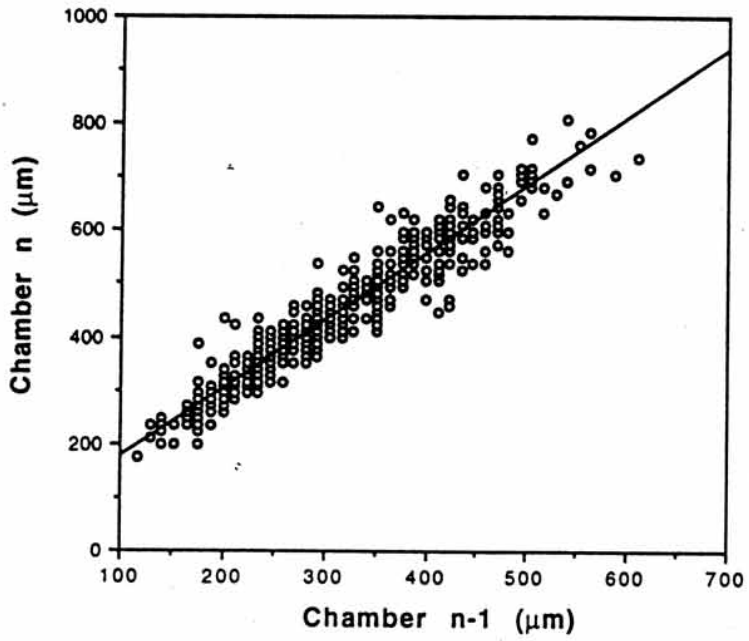

Figure 8: Growth curve of *G. sacculifer*. Best fit regression line is: $D_n = 1.27D_{n-1} + 40$ (for specimens ≥ 100 µm). For explanation see text. Growth below 100 µm was based on measurements from Brummer *et al.* 1987.

$$D_n = 1.27\ D_{n-1} + 48 \text{ (for specimens} \geq 100\ \mu m) \qquad (2)$$

where D_n and D_{n-1} are the diameters for the nth and the (n-1)th chamber-stage respectively. Growth below 100 µm was based on measurements from Brummer *et al.* 1987. 2) The sizeweight function of Anderson and Faber (1984):

$$\text{mass } (\mu g) = 2.89 - 0.0238 * \text{size} + 0.0001 * (\text{size})^2 \qquad (3)$$

is used for size classes ≥ 100 µm. For specimens < 100 µm weight we assume a linear relationship between size and weight. (e.g. a specimen of 40 µm weighs 40% of the weight at 100 µm). 3) The $\delta^{13}C$-depth relationship is based on the data of Figure 7A and, 4) the ontogenetic depth-migration relationships are extracted from Figure 6B:

$$\text{depth (m)} = -0.833 * \text{size} + 83.33 \text{ (for specimens} < 100\ \mu m) \qquad (4a)$$
$$\text{depth (m)} = 0.073 * \text{size} - 4 \text{ (for specimens} \geq 100\ \mu m) \qquad (4b)$$

Using a mass-balance equation (1), the growth relationship (2), the size-weight relationship (3) and the depth migration pattern (4a and 4b), the final $\delta^{13}C$ may be calculated

(Table 1, Figure 9).

To a size of approximately 100 µm, the pre-adult specimens ascend to the surface water, thereby passing the $\delta^{13}C$-maximum at the depth of maximum GAR (gross assimilation rate). After passing the level of maximum GAR, the $\delta^{13}C$ of the test decreases (Figure 9A). During the second part of their life cycle they slowly descend to the reproduction depth, passing the $\delta^{13}C$ maximum again. During the descending phase the $\delta^{13}C$-value initially becomes lighter as long as the $\delta^{13}C$ of ΣCO_2 is still lighter than the test. When they reach a size of ca. 250 µm (at approx. 15 m depth or little deeper) the $\delta^{13}C$ of ΣCO_2 becomes heavier than the value of the test i.e. from there onwards, the test becomes heavier. When the $\delta^{13}C$ maximum in the water column is passed, at an adult test size, the tests become lighter again.

Table 1: Equilibrium $\delta^{13}C$ values (i.e. assuming no biological effect) calculated with a mass balance equation on the basis of ontogenetic migration and a changing ambient $\delta^{13}C_{water}$ with depth.

chamber (#)	shell size (µm)	water depth	$\delta^{13}C$ water	shell weight	chamber weight	$\delta^{13}C$ shell
1	16	70	1.37	0.24	0.24	1.37
2	25	63	1.40	0.38	0.14	1.38
3	28	60	1.41	0.41	0.04	1.38
4	30	58	1.41	0.45	0.04	1.39
5	34	55	1.42	0.51	0.06	1.39
6	37	53	1.41	0.56	0.04	1.39
7	40	50	1.41	0.60	0.05	1.39
8	45	46	1.40	0.68	0.08	1.39
9	52	40	1.38	0.78	0.11	1.39
10	58	35	1.34	0.87	0.09	1.39
11	69	26	1.26	1.04	0.17	1.37
12	75	21	1.20	1.13	0.09	1.35
13	85	13	1.08	1.28	0.15	1.32
14	100	3	0.92	1.51	0.24	1.26
15	175	9	1.02	1.79	0.28	1.22
16	270	16	1.13	3.76	1.97	1.17
17	391	25	1.25	8.88	5.12	1.22
18	545	36	1.35	19.61	10.72	1.29
19	740	50	1.41	40.03	20.42	1.35
20	988	68	1.38	76.95	36.91	1.37

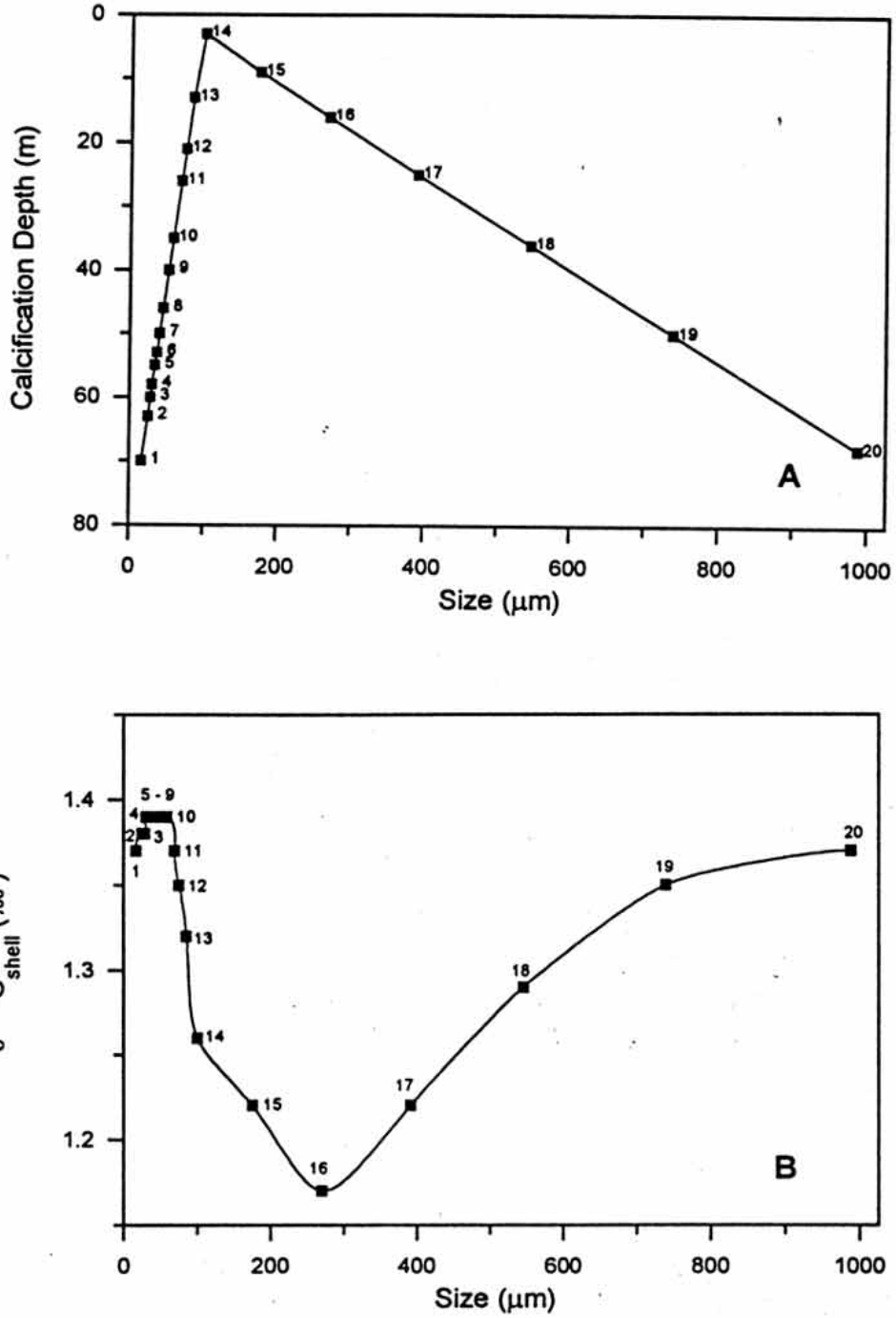

Figure 9: A: The migration of *G. sacculifer* during ontogeny between the surface and approximately 70 m depth. The numbers indicate chamber formation. B: The simulated carbon isotope ratio of the shell of *G. sacculifer* under the assumptions that 1) the $\delta^{13}C$-values of ΣCO_2 of the mixed layer change with depth (see Figure 7A), 2) that *G. sacculifer* migrates up and down in the water column in response to ontogeny, and that 3) chambers are formed in equilibrium with the ambient water (i.e. no vital effect). Chamber numbers are indicated.

DISCUSSION

For comparison, data from Oppo and Fairbanks (1989) were used. On the small size end we added some own measurements from the Red Sea. (Figure 10). This graph demonstrates that the $\delta^{13}C$ of *G. sacculifer* increase with size but that the $\delta^{13}C$ range is much larger than the equilibrium simulation and does not show an increase at smaller sizes (Figure 9A). Apparently, the shells of real foraminifers are not secreted in equilibrium with the ambient seawater and metabolic processes may control the carbon isotope signal and even obscure the ambient value. It has been suggested that $\delta^{13}C$ disequilibrium precipitation of planktic

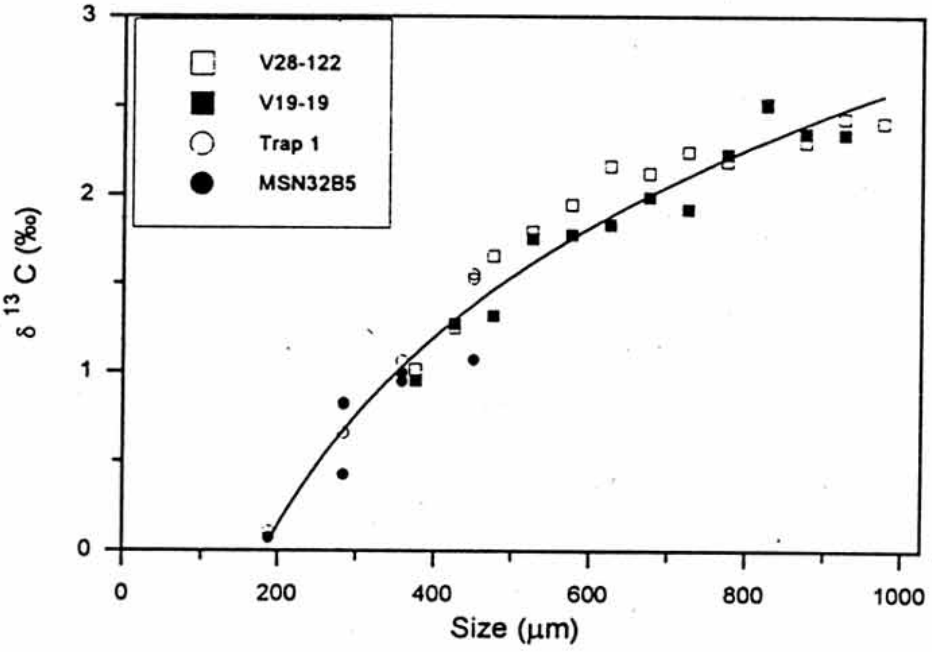

Figure 10: The carbon isotope ratio of *G. sacculifer*. Data from specimens from the Red Sea, collected with multiple o/c net and sediment trap off Barbados, and data from Oppo and Fairbanks (1989) are combined. Best fit is with $\delta^{13}C = -7.96 + 3.52*LOG(size)$.

foraminiferal calcite is controlled by both symbiotic photosynthesis (e.g. Spero and DeNiro, 1987) and foraminiferal respiration (e.g. Berger *et al.*, 1978). The primary sources of HCO_3 for calcification are controlled by diffusion processes between the aqueous environment and the cell (Bé *et al.*, 1981; Anderson and Faber, 1984; Spero and Williams, 1988; Spero *et al.*, 1992). The ΣCO_2 of the seawater between the spines, which may serve as a carbonate pool for calcification, becomes enriched with ^{13}C due to symbiont photosynthesis. As the number of symbionts and/or irradiance levels increase (Figure 11A), the ambient environment will become progressively more enriched. Respiration counteracts

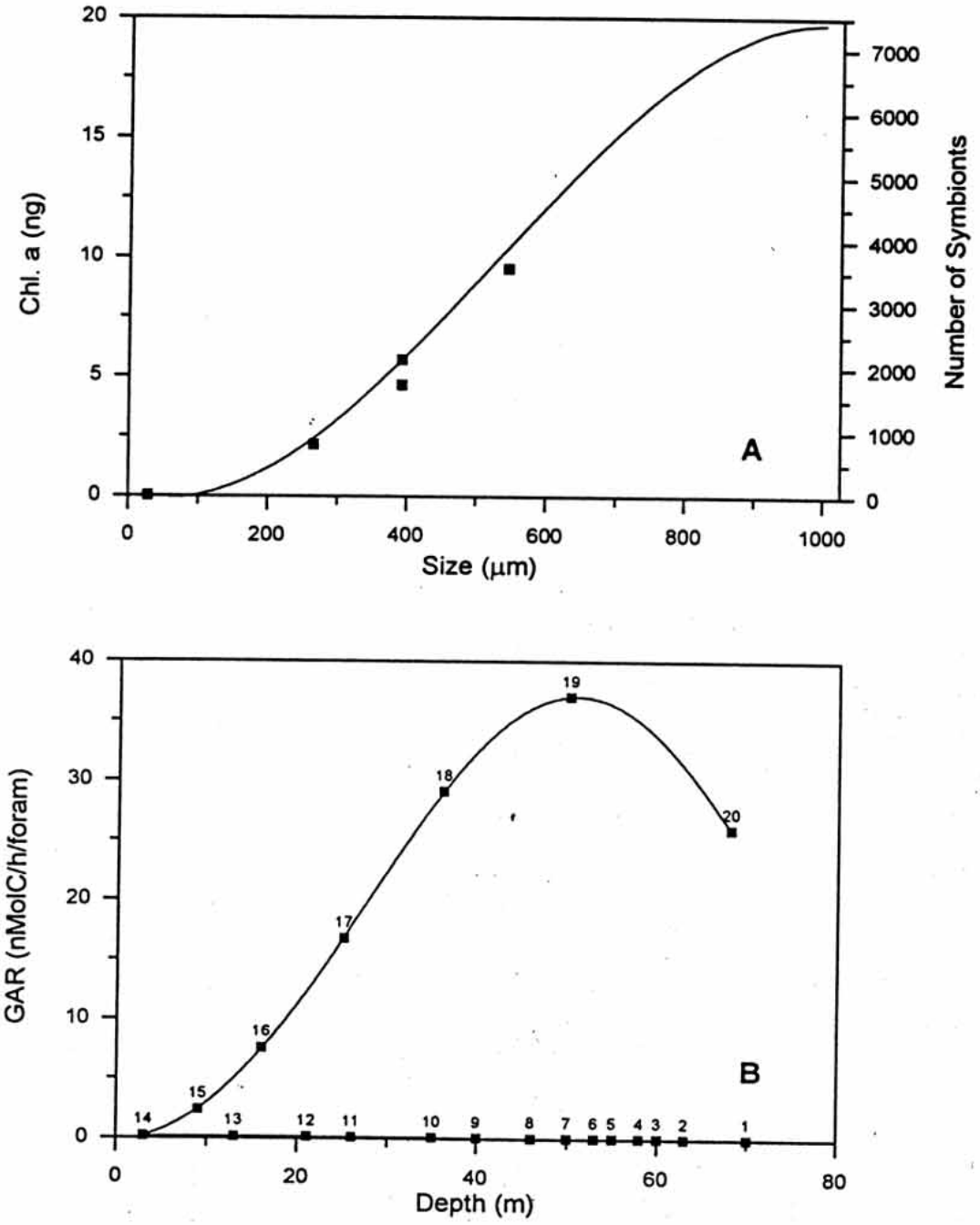

Figure 11: A: Chlorophyll a (square) concentration of *G. sacculifer* as a function of size: Chl. a = 0.191-8E-3*size+7.15E-5*size^2-4.52E-8*size^3. We assume that a symbiont (triangle) contains 2.5 pgChl a/cell (Falkowski and Dubinsky, 1981; McCloskey and Muscatine, 1984) and that 4 symbionts are sequestered at the 3-chamber stage (28 µm). The number of symbionts is plotted at the secondary y-axis. B: The gross assimilation rate of *G. sacculifer* as a function of the ontogenetic migration pattern.

the enrichment by releasing CO_2 derived from light organic compounds to the ambient environment (Spero *et al.*, 1992). ^{13}C-depleted CO_2 may also be released to an internal carbon pool which is used for calcification (Bijma, 1986).

The $\delta^{13}C$ value of the newly formed chamber thus depends on the gross assimilation rate (GAR) and on the respiration rate. The logarithmic trend of the $\delta^{13}C$-size curve (Figure 10) could be explained by (1) a reduction of the photosynthetic activity of the symbionts caused by the change to a deeper habitat in late ontogeny or (2) by an increase of the effect of respiration with size. In order to test this assumption, we modelled the GAR of the symbionts and the respiration of the host-symbiont complex as a function of ontogeny.

GROSS ASSIMILATION RATE.

The GAR is dependent on the number of symbionts and on the light intensity. During the ascending stage of the life cycle, the $\delta^{13}C$ of the test increases rapidly because both, the number of symbionts and the light intensity increase. During the descending phase from early adult stage onwards, the GAR reaches a maximum after which it decreases. Below the depth of maximum GAR, the decrease of the light intensity controls the GAR. Using the sizechlorophyll a plot (Figure 11A), the PI-curve of *G. sacculifer* (Jørgensen *et al.*, 1985) and applying the mass-balance equation, the GAR as a function of depth can be calculated:

$$GAR = P_{max} \cdot \frac{\frac{I_d}{I_k}}{\sqrt{1+\left(\frac{I_d}{I_k}\right)^2}} \qquad (5)$$

where P_{max} is the maximum photosynthetic rate of the symbionts, I_k and I_d are the saturation light intensity of the symbionts and the light intensity at depth d, respectively. The decrease in light intensity with depth is described by the Lambert-Beer equation:

$$I_d = I_0 * d^{(depth * k * z)} \qquad (6)$$

where I_0 is the surface light intensity, k is the extinction coefficient for clear (oligotrophic) open ocean water and z is a factor that compensates for the elevation of the sun. If we assume that the maximum photosynthetic rate (P_{max}) equals 8.17 $pMolO_2$/h,symbiont and that the saturation light intensity (I_k) equals 160 $\mu Em^{-2}sec^{-1}$ (Jørgensen *et al.*, 1985), a surface light intensity of 2000 $\mu Em^{-2}sec^{-1}$, an extinction coefficient of 0.04 (Steemann Nielsen, 1975), and z = 1.2, *G. sacculifer* reaches a maximum GAR of ca. 37 nMolC/h at approximately 50 m

depth (Table 2; Figure 11B). Consequently, the $\delta^{13}C$ value of the test should decrease when the shell continues to calcify below approximately 50 m depth.

RESPIRATION RATE

The $\delta^{13}C$ of oceanic plankton is dependent on their food source. Although consumers reflect the $\delta^{13}C$ of their diet, they are normally slightly enriched (DeNiro and Epstein, 1978). Thus the $\delta^{13}C$ value generally increases towards higher trophic levels in a process which is termed cumulative fractionation (McConnaughey and McRoy, 1979a; 1979b). Depending on the region, copepods were roughly between 2‰ and 5‰ enriched compared the POC (McConnaughey and McRoy, 1979a; Mills *et al.*, 1983; Checkley and Entzeroth, 1985). Nonspinose, herbivorous foraminifers are therefore generally lighter than spinose, carnivorous species (cf. Figure 17 in Vincent and Berger, 1981). Unfortunately, in most reports on the isotopic composition of multiple species from the same environment, the analysis were carried out on different size fractions, making such a comparison invalid. Similarly, the change from juveniles stage in spinose species, feeding on detritus and phytoplankton, to neanic and older stages which have mostly a carnivorous diet, should be accompanied by an increase in the $\delta^{13}C$. Depending on the species, the transition from juvenile to neanic occurs roughly between 60 µm to 80 µm (Brummer *et al.*, 1986, Hemleben *et al.*, 1989). To our knowledge there exist no monospecific isotopic measurements from such small size fractions (pre-neanic), so that this early ontogenetic transition is not documented with isotope data.

Feeding rate also influences the $\delta^{13}C$ of the test. It was shown that the rate of chamber formation and the final size of spinose planktic foraminifers increased proportionally to the feeding frequency (Bé *et al.*, 1981; Hemleben *et al.*, 1987; Bijma *et al.*, 1992). In other words, at a constant temperature and equal size, the respiration rate or metabolic rate is increased at higher feeding rates, which in turn decreases the $\delta^{13}C$-value of the test. Bijma and Hemleben (unpubl. results) found that by doubling the feeding rate of *G. siphonifera*, the $\delta^{13}C$ of the test decreased by approximately 1‰. In contrast, Spero and Lea (in press.) calculated that the respiratory CO_2 accounts for less than 3% of the shell carbon in *G. sacculifer*.

Respiration rate is further dependent on temperature and biomass. We assume a constant temperature, but with increasing biomass, respiration of the foraminifer increases according to the formula of Fenchel and Finlay (1983):

$$\text{respiration (ngC/hr)} = 10^{0.75 * \text{LOG(volume)} - 4.99} \qquad (7)$$

Table 2: The gross assimilation rate and the respiration rate (both in nMolC/hr,foram) are calculated in dependence of number of symbionts, depth migration and size. The difference between these two is expressed as the vital effect (%). The vital effect is maximally 1 ‰.

chamber (#)	size (μm)	depth (m)	LI (μE/m²,s)	Chl. a (ng)	symb. (#)	GAR (nMolC,hr)	volume (μm³)	Resp. (nMolC,hr)	GAR Resp. (nMolC,hr)	Vital effect (%)	unfract. signal (‰)	fract. signal (‰)
1	16	70	69	0.00	0	0.00	8.09	0.00	0.00	0.00	1.37	1.37
2	25	63	100	0.00	0	0.00	3.20	0.00	0.00	0.00	1.38	1.38
3	28	60	110	0.01	4	0.02	4.26	0.01	0.01	0.04	1.38	1.38
4	30	58	122	0.01	4	0.02	5.54	0.01	0.01	0.04	1.39	1.39
5	34	55	143	0.01	5	0.03	8.06	0.01	0.01	0.06	1.39	1.39
6	37	53	161	0.02	6	0.03	1.04	0.02	0.02	0.08	1.39	1.39
7	40	50	181	0.02	7	0.04	1.31	0.02	0.02	0.11	1.39	1.39
8	45	46	221	0.02	8	0.05	1.87	0.02	0.03	0.13	1.39	1.40
9	52	40	293	0.03	10	0.07	2.88	0.03	0.04	0.18	1.39	1.39
10	58	35	372	0.03	12	0.09	4.00	0.04	0.05	0.22	1.39	1.39
11	69	26	578	0.04	15	0.12	6.73	0.06	0.06	0.27	1.37	1.37
12	75	21	735	0.05	18	0.14	8.65	0.07	0.07	0.33	1.35	1.36
13	85	13	1096	0.05	20	0.16	1.26	0.08	0.07	0.33	1.32	1.32
14	100	3	1707	0.06	24	0.20	2.05	0.12	0.08	0.34	1.26	1.26
15	175	9	1313	0.74	295	2.40	1.10	0.59	1.81	7.79	1.22	1.30
16	270	16	940	2.36	943	7.60	4.05	1.69	5.91	25.46	1.17	1.43
17	391	25	615	5.30	2119	16.76	1.23	3.85	12.90	55.64	1.22	1.77
18	545	36	359	9.75	3899	29.10	3.32	7.66	21.44	92.47	1.29	2.22
19	740	50	181	15.11	6046	37.03	8.31	13.84	23.19	100.00	1.35	2.36
20	988	68	76	18.51	7403	25.97	1.98	23.10	2.87	12.40	1.37	1.49

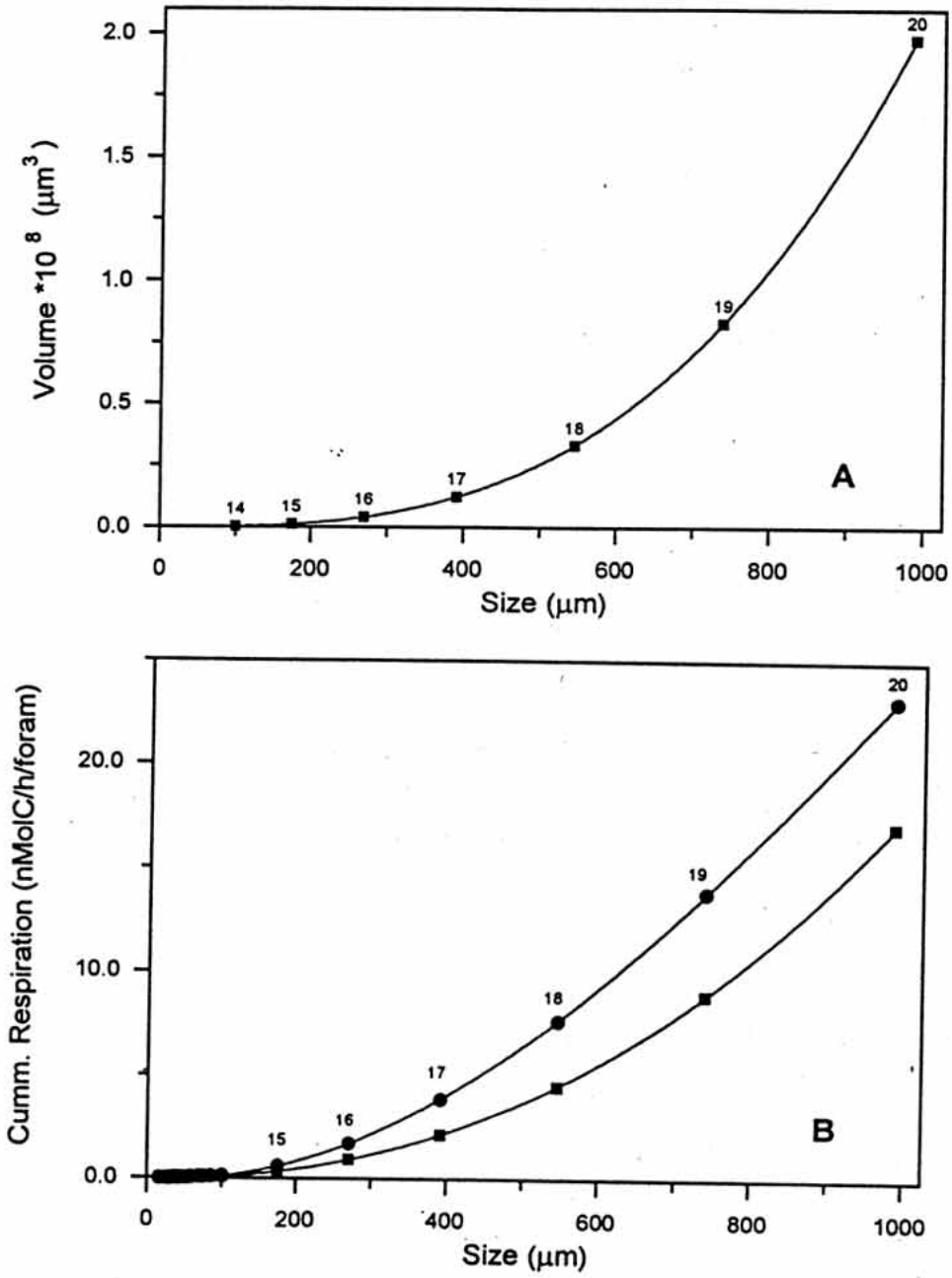

Figure 12: A: The volume of *G. sacculifer* calculated with the method of Ott *et al.* (1992): V = 0.205 * size^3. B: The cumulative respiration rate (square: host respiration; circle: symbiont respiration) as a function of size. The equation of Fenchel and Finlay (1983) was modified to fit *G.sacculifer*. The numbers denote chambers.

The volume increases with increasing size (Figure 12A). As a rule of thumb, respiration of the symbionts is usually considered to dissipate some 10% of the gross primary production achieved at saturation (e.g. Barnes and Hughes, 1982). In late ontogeny, the total respiration reaches the same order of magnitude as the photosynthesis of the symbionts (table 2). As the total respiration increases, the internal carbon pool and the ambient environment receive more ^{12}C and the $\delta^{13}C$-value of the test decreases.

THE OVERALL VITAL EFFECT

The effect of photosynthesis raises and the effect of respiration lowers the $\delta^{13}C$-size curve (Figure 6B). The biochemical pathways that deliver the carbon may be different as well. For instance, if carbon from the internal carbon pool (depleted by respiration) is the dominant source for calcification, the effect of respiration is important. If, on the other hand, epitactic growth is the predominant process, symbiont photosynthesis may be the most important process because carbon from the ambient environment (enriched by photosynthesis) will be used. We assume that both processes affect the carbon isotope value of the shell to an equal extent, i.e. in relation to their absolute carbon turnover rates. Consequently, we can estimate the vital effect by subtracting the absolute carbon release by respiration from the absolute carbon fixation by the symbionts. The relative vital effect at each ontogenetic stage can now be calculated by setting the maximum absolute change in carbon equal to 100 % vital effect (Figure 13A). Apparently, the vital effect is negligible in early ontogeny. Afterwards it tends to increase the $\delta^{13}C$-value of the shell. It reaches a maximum between the 18th and 19th-chamber stage. At the end of the life cycle the effect of the vital processes is to reduce the $\delta^{13}C$ of the shell. In the present simulation experiment we allow a vital effect for the carbon isotopes that is two times as strong as that for oxygen isotopes (ca. 0.5‰ e.g. Hemleben *et al.*, 1989). An increase between 1 and 2‰, in the carbon isotope composition due to light intensity alone was reported by Spero (1988) and Spero and Deniro (1987) respectively. A decrease of about 1‰, was found at higher feeding frequency in *G. siphonifera* (Bijma *et al.*, unpub. results). In other words, a vital effect of about 1‰, is very realistic for carbon isotopes. The resulting change of the $\delta^{13}C$ of the shell with ontogeny can be calculated (Figure 13B). Thus the vital effect tends to amplify the shape of the equilibrium signal that results from the migratory pattern (cf. Figure 13B with Figure 9B). Depending on local conditions, the shapes of the curve may of course vary, just as the amplitude.

Several arguments, indicate that photosynthesis of the symbionts may not be such an important controlling mechanism for carbon fractionation as we assume here: 1) *G. siphonifera* cultured in continuous darkness show the same trend as specimens cultured under light, although the slope may be slightly less inclined (Bijma and Hemleben, unpublished results). 2) Spinose non-symbiotic species such as e.g. *G. bulloides* also show the same general pattern of figure 10. 3) Chamber formation (calcification) in *G. sacculifer* predominantly occurs between 6 p.m. and 12 p.m. (Bijma, 1986).

If only host-symbiont respiration is considered the shape of the curve becomes even further away from reality. We therefore conclude that more information on the mechanisms that control foraminiferal $\delta^{13}C$ is needed before the carbon isotope black box can really be opened.

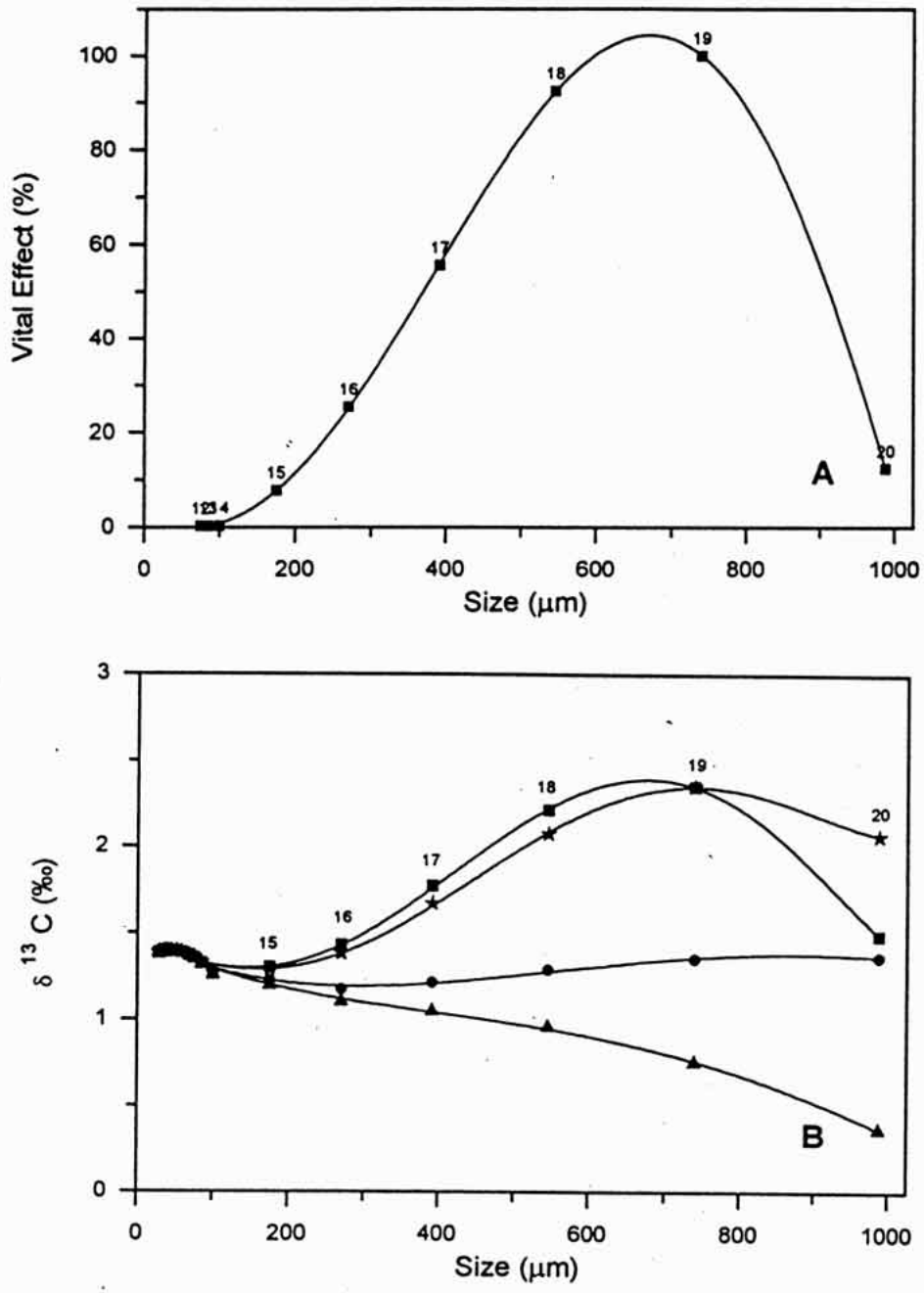

Figure 13 A: The difference between the GAR and the total respiration expressed as percent vital effect. B: The $\delta^{13}C$ as a function of ontogeny if vital effect is included. The maximum effect of the vital processes on the $\delta^{13}C$ of the shell is assumed to be 1 ‰ (circle: original signal; asterisk: fract. (G); triangle: fract. (R); square: fract. (G-R)).

ACKNOWLEDGEMENTS

We thank Ingrid Breitinger and Rolf Ott for their helpful assistance and Howard Spero and Fred Banner for critical remarks that improved the manuscript. The authors acknowledge the editor's engagement in both the meeting and assembling the volume.

REFERENCES

ANDERSON, O.R., FABER, W.W., Jr., 1984. An estimation of calcium carbonate deposition rate in planktonic foraminifera *Globigerinoides sacculifer* using 45-Ca as a tracer: a recommended procedure for improved accuracy. J. Foram. Res., 14, 303-308.

ALMOGI-LABIN, A., 1984, Population dynamics of planktic Foraminifera and Pteropoda - Gulf of Aqaba, Red Sea: Proc. Koninkl. Nederlandse Akad. Wetensch., Ser. B, 87, 4, 481-511.

BARNES, RSK, HUGHES, RN, 1982. Introduction to Marine Ecology, Blackwell Scientific Publications, 339 p.

BÉ, A.W.H. CARON, D.A., ANDERSON, O.R., 1981, Effects of feeding frequency on life processes of the planktonic foraminifer Globigerinoides sacculifer in laboratory culture: J. Mar. Biol. Assoc. U.K., 61, 257-277.

BERGER, W.H. KILLINGLEY, J.S., VINCENT, E., 1978, Stable isotopes in deep-sea carbonates: Box Core ERDC-92 west equatorial Pacific: Oceanol. Acta, 1, 2, 203-216.

BIJMA, J., 1986, Observations on the life history and carbon cycling of planktonic foraminifera from the Gulf of Elat/Aqaba. Unpubl. Master Thesis, Univ. Groningen, The Netherlands, 120 p.

BIJMA, J., J. EREZ, HEMLEBEN Ch., 1990, Lunar and semi-lunar reproductive cycles in some spinose planktonic foraminifers. Journal of Foraminiferal Research, 20 (2), 117-127.

BIJMA, J., HEMLEBEN Ch., 1993, Population dynamics of *G. sacculifer* (Brady) from the Central Red Sea: Deep Sea Res.

BIJMA, J., Ch. HEMLEBEN, H. OBERHÄNSLI, SPINDLER M., 1992. The effects of increased water fertility on tropical spinose planktonic foraminifers in laboratory cultures: J. Foram. Res., 22,3, 242-256.

BRUMMER, G.J., HEMLEBEN Ch., SPINDLER M., 1987. Ontogeny of extant spinose planktonic foraminifera (Globigerinidae): A concept exemplified by *G. sacculifer* (Brady) and *G. ruber* (d'Orbigny). Mar. Micropal., 2, 357-381.

BROECKER, W.S., MAIER-REIMER E, 1992. The influence of air and sea exchange on the carbon isotope distribution in the sea: Global Biogeochemical Cycles, 8(3), 315-320.

CHECKLEY, D.M., ENTZEROTH L.C., 1985. Elemental and isotopic fractionation of carbon and nitrogen by marine, planktonic copepods and implications to the marine nitrogen cycle: J. Plankt. Res., v. 7(4), 553-568.

DENIRO, M.J., EPSTEIN, S., 1978. Influence of diet on the distribution of carbon isotopes in animals: Geochim. and Cosmochim. Acta, v. 42, 495-506.

EREZ, J., A. ALMOGI-LABIN, AVRAHAM S., 1991, Lunar Reproduction Cycle in *Globigerinoides sacculifer* (Brady). Paleoceanography, 6 (3), 295-306.

FALKOWSKI, P.G., DUBINSKY Z., 1981. Light-shade adaptation of *Stylophora pistilata,* a hermatypic coral from the Gulf of Eilat. Nature, v. 289, p. 172-174.

FENCHEL, T., FINLAY B.J., 1983, Respiration rates in heterotrophic, free-living protozoa. A review. Microb. Ecol., v. 9, 99-122.

HEMLEBEN, CH., M. SPINDLER, ANDERSON O.R., 1989, Modern Planktonic Foraminifera, Springer Verlag, 363 pp.

HEMLEBEN, CH. SPINDLER, M. BREITINGER, I., OTT, R., 1987, Morphological and physiological responses of Globigerinoides sacculifer (Brady) under varying laboratory

conditions: Marine Micropal., 12, 305-324

JØRGENSEN, B.B. EREZ, J. REVSBECH, N.P., COHEN, Y., 1985, Symbiotic photosynthesis in a planktonic foraminiferan, Globigerinoides sacculifer (Brady), studied with microelectrodes: Limnol. Oceanogr., 30, 1253-1267

McCLOSKEY, L.R., MUSCATINEL., 1984. Production and respiration in the Red Sea coral Stylophora pistillata as a function of depth. Proc. of the Royal Soc, London, B222, 215.230.

McCONNAUGHEY, T., MCROY, C.P., 1979a. Foodweb structure and the fractionation of carbon isotopes in the Bering Sea. Mar. Biol., 53, 257-262.

McCONNAUGHEY, T., MCROY, C.P., 1979b. ^{13}C label identifies eelgrass (*Zostera marina*) carbon in the alaskan estuari foodweb. Mar. Biol., 53, 263-269.

MILLS, E.L., K. PITTMAN and F.C. TAN, 1983. Food web structure on the Scotian shelf, eastern Canada. study using ^{13}C as a food chain tracer. ICES. Rapp. Proc. Verb. Reun., 183, 111-118.

OTT, R., J. BIJMA, Ch. HEMLEBEN and M. SIGNES, 1992, A computer method for estimating volumes and surface areas of complex structures consisting of overlapping spheres. Math. Comput. Modelling, 16(12), 83-98.

REISS, Z., and L. HOTTINGER (1984) The Gulf of Aqaba. Ecological Micropaleontology. Ecological studies 50. Springer-Verlag, Berlin, Heidelberg, New York and Tokyo, 354p.

SPERO, H.J. and M.J. DENIRO, 1987, The influence of symbiont photosynthesis on the $\delta^{13}O$ and $\delta^{13}C$ values of planktonic foraminiferal shell calcite. Symbiosis, 4, 213-228.

SPERO, H.J. and D.W. LEA, in press., Intraspecific stable isotope variability in the planktonic foraminifera *Globigerinoides sacculifer*: Results from laboratory experiments. Mar. Micropal.

SPERO, H.J. and D.F. WILLIAMS, 1988. Extracting environmental information from planktonic foraminiferal $\delta^{13}C$ data. Nature, 335, 717-719.

SPERO, H.J. and D.F. WILLIAMS, 1989. Opening the carbon isotope "vital effect" black box, I: Seasonal temperatures in the euphotic zone. Paleoceanography, 4, 593-601.

SPERO, H.J., LERCHE, I. and D.F. WILLIAMS, 1992. Opening the carbon isotope "vital effect" black box, 2; Quantitative model for interpreting foraminiferal carbon isotope data. Paleoceanography, 6, 639-655.

STEEMANN NIELSEN, E., 1975. Marine photosynthesis. With special emphasis on the ecological aspects. Elsevier Scientific Publishing company, Amsterdam, 141 p.

SPINDLER, M., Ch. HEMLEBEN, U. BAYER, A.W.H. BÉ and O.R. ANDERSON, 1979, Lunar Periodicity of Reproduction in the Planktonic Foraminifer *Hastigerina pelagica*. Marine Ecology, Progress Series 1, 1, 61-64.

VINCENT, E., and BERGER, W.H. 1981. Planktonic foraminifera and their use in paleooceanography. In: The oceanic lithosphere, The Sea. C. Emiliani (ed.), v. 7, 1025-1119.

WILLIAMS, D.F. SOMMER, M.A. and BENDER, M.L., 1977, Carbon isotopic compositions of Recent planktonic Foraminifera of the Indian Ocean: Earth Planet. Sci. Lett., v. 36, 391-403.